Fibrillar amyloid-β burden in cognitively normal people at 3 levels of genetic risk for Alzheimer's disease

Eric M. Reiman[a,b,c,d,1], Kewei Chen[a,d,e,f], Xiaofen Liu[a,d], Daniel Bandy[a,d], Meixiang Yu[a,d,g], Wendy Lee[a,d], Napatkamon Ayutyanont[a,d], Jennifer Keppler[a,d], Stephanie A. Reeder[a,d], Jessica B. S. Langbaum[a,d], Gene E. Alexander[d,h], William E. Klunk[i], Chester A. Mathis[j], Julie C. Price[j], Howard J. Aizenstein[i], Steven T. DeKosky[i,k,2], and Richard J. Caselli[d,l]

[a]Banner Alzheimer's Institute and the Positron Emission Tomography Center, Good Samaritan Regional Medical Center, Phoenix, AZ 85006; Departments of [b]Psychiatry, [e]Radiology, and [h]Psychology and Evelyn F. McKnight Brain Institute, University of Arizona, Tucson, AZ 85721; [c]Neurogenomics Division, Translational Genomics Research Institute, Phoenix, AZ 85004; [f]Department of Mathematics and [g]Biodesign Institute, Arizona State University, Tempe, AZ 85287; Departments of [i]Psychiatry, [k]Neurology, and [j]Radiology, University of Pittsburgh, Pittsburgh, PA 15260; [l]Department of Neurology, Mayo Clinic Arizona, Scottsdale, AZ 85259; and the [d]Arizona Alzheimer's Consortium, Phoenix, AZ 85006

Fibrillar amyloid-beta (Aβ) is found in the brains of many cognitively normal older people. Whether or not this reflects a predisposition to Alzheimer's disease (AD) is unknown. We used Pittsburgh Compound B (PiB) PET to characterize the relationship between fibrillar Aβ burden and this predisposition in cognitively normal older people at 3 mean levels of genetic risk for AD. Dynamic PiB PET scans, the Logan method, statistical parametric mapping, and automatically labeled regions of interest (ROIs) were used to characterize and compare cerebral-to-cerebellar PIB distribution volume ratios, reflecting fibrillar Aβ burden, in 28 cognitively normal persons (mean age, 64 years) with a reported family history of AD and 2 copies, 1 copy, and no copies of the apolipoprotein E (APOE) $\varepsilon 4$ allele. The 8 $\varepsilon 4$ homozygotes, 8 heterozygotes, and 12 noncarriers did not differ significantly in terms of age, sex, or cognitive scores. Fibrillar Aβ was significantly associated with APOE $\varepsilon 4$ carrier status and $\varepsilon 4$ gene dose in AD-affected mean cortical, frontal, temporal, posterior cingulate-precuneus, parietal, and basal ganglia ROIs, and was highest in an additional homozygote who had recently developed mild cognitive impairment. These findings suggest that fibrillar Aβ burden in cognitively normal older people is associated with APOE $\varepsilon 4$ gene dose, the major genetic risk factor for AD. Additional studies are needed to track fibrillar Aβ accumulation in persons with different kinds and levels of AD risk; to determine the extent to which fibrillar Aβ, alone or in combination with other biomarkers and risk factors, predicts rates of cognitive decline and conversion to clinical AD; and to establish the role of fibrillar Aβ imaging in primary prevention trials.

apolipoprotein E | Pittsburgh Compound B PET

Fibrillar amyloid-beta (Aβ) deposition is a cardinal neuropathological feature of Alzheimer's disease (AD), the major constituent of neuritic plaques, and used in the postmortem diagnosis of cognitively impaired patients. The "amyloid cascade" hypothesis suggests that certain soluble or fibrillar Aβ species are critically involved in the early pathogenesis of AD (1), that fibrillar Aβ accumulation begins before cognitive decline (2), and that Aβ-modifying treatments now in development may be most effective if initiated before significant Aβ neuropathology or symptoms become established (3). Postmortem neuropathological studies find significant fibrillar Aβ burden in many older people who were cognitively normal (2, 4, 5). Antemortem brain imaging studies are needed to determine the extent to which fibrillar Aβ in cognitively normal people predicts the subsequent development of clinical AD.

[11]C-labeled Pittsburgh Compound B (PiB) is a PET radioligand that selectively binds to fibrillar aggregates of the Aβ peptide (6, 7). PiB and other recently developed radioligands for the assessment of fibrillar Aβ in the living human brain have been used to confirm the presence of significant fibrillar Aβ in many cognitively older normal persons (6, 8–11). They are now being used in longitudinal studies to determine the extent to which asymptomatic fibrillar Aβ burden, alone or in combination with other risk factors and measurements, predicts subsequent rates of cognitive decline and clinical conversion to mild cognitive impairment and AD (12). As a complement to longitudinal studies, we sought to determine whether fibrillar Aβ in cognitively normal persons is associated with a predisposition to AD by comparing individuals at different levels of genetic risk.

The apolipoprotein E (APOE) $\varepsilon 4$ allele is the major susceptibility gene in persons with AD with onset of dementia after age 60. Each additional copy of the $\varepsilon 4$ allele in a person's APOE genotype (i.e., APOE $\varepsilon 4$ gene dose) is associated with a greater risk of AD and a younger median age at onset of dementia, and $\varepsilon 4$ homozygotes are an especially high risk (13–16). For example, in the original case-control study, AD risk and mean age at clinical onset were 91% and 68 years in $\varepsilon 4$ homozygotes, 47% and 76 years in heterozygotes, and 20% and 84 years in noncarriers (14). Although these values need to be refined by population-based cohort studies initiated before the age of AD risk, the reported relationship between APOE $\varepsilon 4$ gene dose and AD is very strong (15, 16).

In an ongoing longitudinal study, we have been using fluorodeoxyglucose PET, volumetric MRI, clinical rating scales, and neuropsychological tests to follow initially late–middle-aged, cognitively normal $\varepsilon 4$ homozygotes, heterozygotes, and noncarriers every 2 years. We previously found that compared with noncarriers, $\varepsilon 4$ carriers have a significantly lower cerebral glucose metabolism in the same brain regions as patients with

Table 1. Subject characteristics, clinical ratings, and neuropsychological test scores

Characteristic, rating, or test score	Noncarriers ($n = 12$)	Heterozygotes ($n = 8$)	Homozygotes ($n = 8$)	P value
Age, years	64 ± 5 (57–71)	67 ± 4 (60–72)	63 ± 4 (60–71)	.14
Females/males	9 / 3	7 / 1	5 / 3	.51
Educational level, years	15 ± 2	17 ± 2	15 ± 2	.02
MMSE score	29.7 ± 0.7 (28–30)	29.6 ± 1.1 (27–30)	29.6 ± 0.7 (28–30)	.99
Auditory verbal learning test scores				
Total learning	48.1 ± 6.2	50.9 ± 11.2	47.4 ± 11.8	.74
Short-term recall	9.1 ± 2.7	10.0 ± 3.5	9.4 ± 4.2	.84
Long-term recall	8.5 ± 3.3	10.6 ± 3.8	8.5 ± 4.0	.40
Complex figure test scores				
Copy	34.5 ± 2.0	32.5 ± 3.9	35.4 ± 0.9	.08
Recall	19.4 ± 7.3	21.2 ± 9.3	19.8 ± 6.5	.88
Boston naming test	56.4 ± 2.9	56.6 ± 4.0	57.0 ± 2.5	.92
Wechsler Adult Intelligence Scale-Revised scores				
Information	14.3 ± 7.1	13.3 ± 3.0	12.3 ± 1.8	.69
Digit span	11.3 ± 2.4	12.8 ± 3.5	12.0 ± 2.3	.53
Block design	12.6 ± 2.7	12.4 ± 2.9	13.0 ± 3.1	.91
Mental arithmetic	11.8 ± 2.2	12.1 ± 3.4	13.3 ± 2.5	.51
Similarities	11.8 ± 1.5	13.3 ± 3.2	13.5 ± 1.6	.18
Controlled oral word association test	47.5 ± 11.8	53.6 ± 10.6	49.8 ± 2.5	.40
Wechsler Memory Scale-Revised Orientation subtest score	14.0 ± 0.0	13.9 ± 0.4	13.8 ± 0.5	.22

Values are means ± SD with ranges in parentheses as appropriate. P values were calculated using the unpaired 2-tailed t-tests or 2-tailed Pearson χ^2 test, uncorrected for multiple comparisons.

probable AD (17, 18), which is progressive (19) and significantly correlated with $\varepsilon4$ gene dose (i.e., 3 levels of AD risk) (20), and can be detected in young adults as well (21). Having recently begun to acquire PiB PET images in these subjects, we sought to characterize the relationship between fibrillar Aβ burden in cognitively normal persons and these 3 levels of genetic risk for AD. Based in part on our findings, in this paper we discuss the potential role of fibrillar Aβ imaging in the preclinical detection and tracking of AD, the assessment of other AD risk factors, and the evaluation of putative risk-reduction and prevention therapies.

Results

The cognitively normal $\varepsilon4$ homozygotes, heterozygotes, and noncarriers in this study did not differ significantly in terms of age, sex distribution, MiniMental State Examination (MMSE) score, or neuropsychological test scores (Table 1). The heterozygotes had a slightly higher educational level compared with the other 2 groups. As noted in *Materials and Methods*, an additional $\varepsilon4$ homozygote developed subjective and neuropsychological evidence of cognitive decline in the 2 years between her last 2 clinical visits, and she was diagnosed with amnestic mild cognitive impairment (MCI) 7 months before her PiB scan.

Based on the analysis of the data from our cognitively normal subjects' mean cortical region-of-interest (ROI) and their other standardized ROIs, average PiB distribution volume ratios (DVRs) increased progressively with each additional $\varepsilon4$ allele (Fig. 1). Average DVRs in the previously studied probable AD group were even higher, whereas the DVR in the homozygote who developed MCI was higher than in all of the cognitively normal subjects and similar to those in the probable AD group. Analyzing data from the 28 cognitively normal subjects, fibrillar Aβ burden was significantly associated with *APOE* $\varepsilon4$ gene dose in mean cortical, frontal, posterior cingulate-precuneus, temporal, parietal, and basal ganglia ROIs ($P < .05$; 2-tailed linear trend, Bonferroni-corrected). The homozygotes had significantly higher measurements than the noncarriers ($P < .05$; 2-tailed ANOVA with pairwise comparisons, Bonferroni-corrected) and nonsignificant trends for higher measurements

compared with the heterozyotes ($.02 < P < .20$; 2-tailed, uncorrected for multiple comparisons) in each of these ROIs. The heterozygotes had nonsignificant trends for higher measurements compared with the noncarriers in mean cortical, frontal, posterior cingulate-precuneus, and basal ganglia ROIs ($.05 < P < .11$; 2-tailed, uncorrected for multiple comparisons). The association between higher PiB DVR and *APOE* $\varepsilon4$ gene dose, along with the higher DVR in the homozygote with MCI and in patients with probable AD, support the likelihood that fibrillar Aβ deposition in these $\varepsilon4$ carriers will increase further before the possible onset of MCI or dementia. Within each ROI, PiB DVRs from the previously studied $\varepsilon4$ homozygote, heterozygote, and noncarrier probable AD patients did not differ significantly (e.g., mean cortical DVR, 1.8 ± 0.3, 1.8 ± 0.1, and 1.9, respectively; $P = .87$, ANOVA), and were similar to the DVR in the homozygote with MCI. In the homozygote group, mean cortical PiB DVRs were lowest in the 2 youngest subjects (age 60 and 61) and highest in the oldest subject (age 73), who had recently developed MCI (Fig. 1), and were correlated with age ($R = 0.79$; $P = .01$). Indeed, correlations between mean cortical PiB DVR and age were significantly greater in the homozygotes compared with the noncarriers whether or not the data from the homozygote with MCI were included ($P = .002$ and .03, respectively). Using our predefined criteria for PiB-positivity, none of the $\varepsilon4$ noncarriers, half of the heterozygotes, two-thirds of the homozygotes (including the one with MCI), and all of the probable AD patients were PiB-positive.

As revealed by the statistical brain map analyses (Fig. 2A–C and Table 2), *APOE* $\varepsilon4$ heterozygotes had significantly higher PiB DVRs than noncarriers in frontal, anterior, middle, posterior cingulate, temporal, parietal, and basal ganglia locations; homozygotes had higher measurements than noncarriers in even more extensive bilateral locations; and PiB DVRs in these extensive locations were associated with *APOE* $\varepsilon4$ gene dose. Conversely, there were no cerebral locations in which PiB DVR was higher in the noncarrier group than in either the heterozygote or homozygote group, and there were no cerebral locations in which PiB DVR was inversely associated with *APOE* $\varepsilon4$ gene dose, even at the liberal significance threshold of $P < .05$ (uncor-
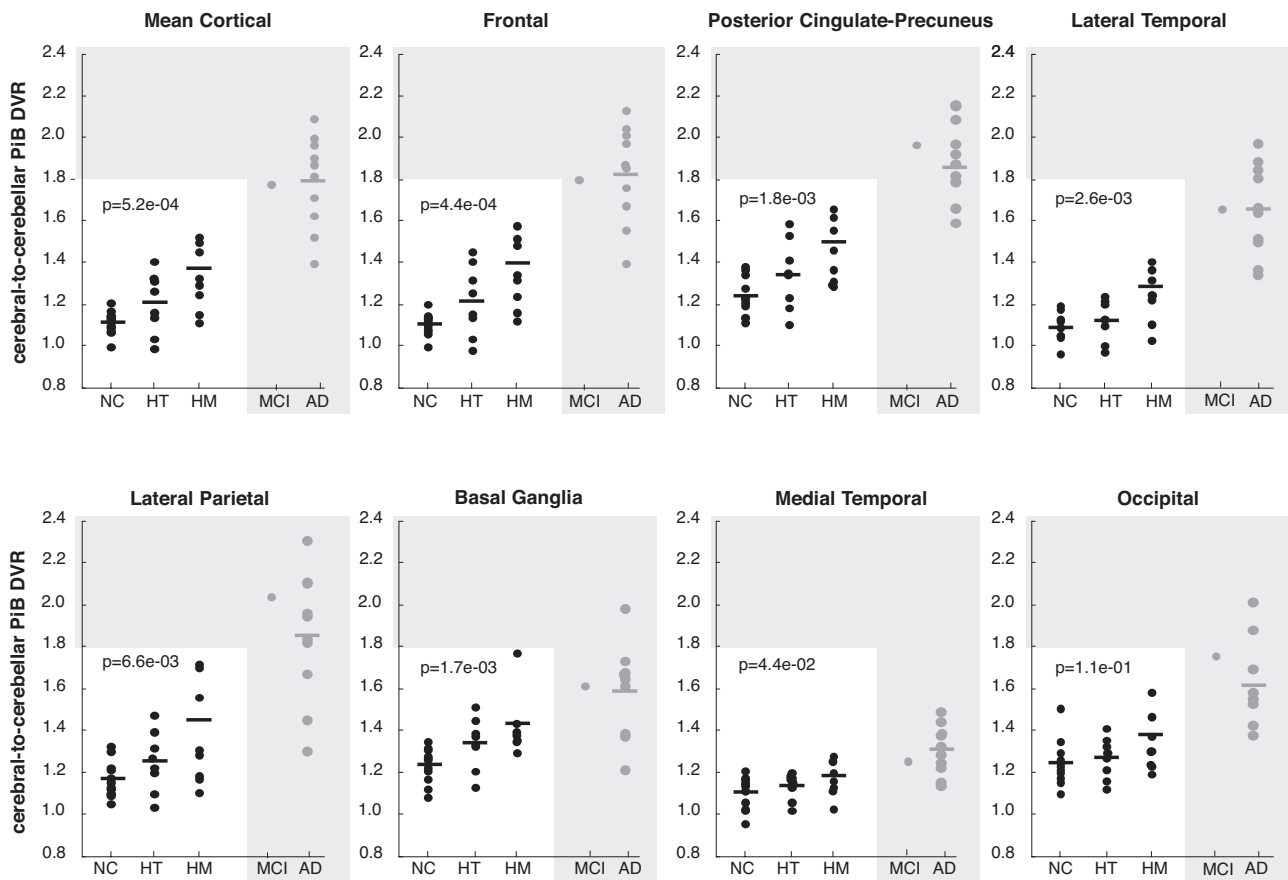
Fig. 1. Fibrillar Aβ burden in cognitively normal *APOE ε*4 noncarriers (NC), heterozygotes (HT), and homozygotes (HM) from our longitudinal study (white box), an HM with recent onset of MCI, and probable AD patients from a previous study (gray box). The data were generated from the ROIs shown in Fig. 3. The mean value in the HM group and statistical analyses in the text do not include data from the HM with MCI. *P* values correspond to the association between fibrillar Aβ burden and *APOE ε*4 gene dose (2-tailed linear trend) in the cognitively normal subjects.

rected for multiple comparisons). Indeed, the number of cerebral voxels associated with higher PiB DVR in the heterozygote–noncarrier, homozygote–noncarrier, homozygote–heterozygote, and ε4 gene dose comparisons at *P* <.05 (uncorrected for multiple comparisons) was much higher than that associated with lower PiB DVR in each of the respective comparisons (*P* < e-16; χ^2test).

Discussion

This study demonstrates an association between fibrillar Aβ burden in cognitively normal individuals at 3 levels of genetic risk for AD. *APOE ε*4 gene dose, the major genetic risk factor for AD cases with onset of dementia after age 60, was associated with higher fibrillar Aβ in a mean cortical ROI; frontal and posterior cingulate-precuneus and temporal, parietal, and basal ganglia ROIs; and other cerebral locations known to be affected in symptomatic patients. The homozygote with MCI had an even greater fibrillar Aβ burden, comparable to the average in patients with probable AD.
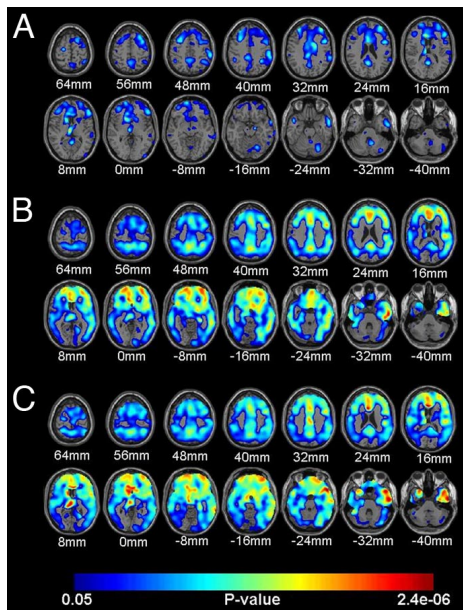
The cognitively normal homozygotes, heterozygotes, and noncarriers from our ongoing longitudinal study were demographically well matched, had high MMSE and neuropsychological test scores, and tended to be somewhat younger than the cognitively normal subjects in previously reported neuropathological and brain imaging studies (2, 4, 6, 8–10). By directly comparing cognitively normal individuals with differing levels of AD risk, we were able to detect potentially modest increases in fibrillar Aβ in cognitively normal people without the need for to use a

minimum Aβ threshold. Because the classification of subjects as "PiB-positive" or "PiB-negative" may be a useful way to address certain other scientific and clinical questions, we also report that none of the cognitively normal ε4 noncarriers, half of the heterozygotes, and two-thirds of the homozygotes (including the one with MCI) could be classified as PiB-positive.

Recently, several of our group used PiB PET to demonstrate fibrillar Aβ burden in 5 asymptomatic presenilin 1 (PS1) mutation carriers from a kindred with dominantly inherited early-onset AD, 3 of whom performed within the normal range on all neuropsychological tests and who were 6–13 years younger than the kindred's reported mean age at symptomatic onset (22). The pattern of fibrillar Aβ burden in the asymptomatic PS1 carriers, and also in the symptomatic PS1 carriers from another kindred, was characterized by much higher deposition in the striatum than in the cerebral cortex, different from the less prominent striatal deposition in older persons with or without probable AD. In contrast, the pattern of fibrillar Aβ burden in each of our cognitively normal *APOE ε*4 carrier groups was similar to that in older persons with and without AD.

The present study used PiB DVR measurements from automatically characterized and spatially standardized cerebral and cerebellar reference ROIs to facilitate the comparison of measurements from different subjects and findings from different laboratories, while reducing type 1 error. For instance, the mean cortical-to-cerebellar Aβ measurement could be used by different laboratories in the early detection and tracking of AD, as a quantitative endophenotype for the presymptomatic assessment

Reiman et al.

Fig. 2. Statistical brain maps showing higher cerebral-to-cerebellar PiB DVR, a measure of fibrillar Aβ, in the 8 cognitively normal *APOE* ε4 heterozygotes (*A*) and the 8 cognitively normal homozygotes (*B*) compared with the 12 cognitively normal noncarriers, and associations between higher PiB DVR and *APOE* ε4 gene dose in the 28 cognitively normal subjects (*C*). Statistical maps are superimposed onto horizontal sections from a spatially standardized MRI image and are shown in relationship to their distance above or below a horizontal plane through the anterior and posterior commissures.

of putative genetic and nongenetic AD risk factors (particularly risk factors thought to contribute to Aβ pathology) (20, 21, 23), and as an endpoint for evaluating putative Aβ-modifying treatments in prevention trials (24), without statistical correction for multiple comparisons. The study also used statistical brain maps to characterize the pattern and magnitude of fibrillar Aβ burden

in persons at risk for AD, compare them with the pattern and magnitude in symptomatic AD patients, and explore fibrillar Aβ deposition with greater anatomical precision and sensitivity than can be achieved by using preselected ROIs, which depend in part on their size and location.

In the cognitively normal subjects, fibrillar Aβ burden was correlated with *APOE* ε4 gene dose, was significantly greater in the 2 ε4 carrier groups compared with the noncarriers, and was significantly lower than in persons with probable AD or in the homozygote with MCI. Based on these findings, we predict that fibrillar Aβ in cognitively normal persons with this major genetic risk factor will increase further before the onset of MCI or dementia, providing a marker of disease progression that could be used in AD prevention trials.

Although we have found an association between fibrillar Aβ in cognitively normal *APOE* ε4 carriers, other studies have identified older individuals without the *APOE* ε4 allele who are PiB-positive. The *APOE* ε4 allele is associated with increased cerebral and vascular Aβ deposition in AD (25), and the ApoE E4 isoform is associated with increased Aβ binding, fibrillization, and cerebral and vascular Aβ deposition (13, 26), as well as with decreased ApoE-mediated Aβ clearance and degradation (27–29). Preliminary studies have raised the possibility that ε4 carriers and noncarriers may respond differently to certain treatments (30). For these and other reasons, it will be important to characterize and compare the extent to which fibrillar Aβ in cognitively normal *APOE* ε4 carriers and noncarriers is related to the predisposition to late-onset AD.

Limitations of the present study include the relatively small number of subjects; the restriction of comparisons to persons with a reported family history of probable AD; the inability of PiB to assess soluble (including oligomeric) forms of Aβ, some of which have been postulated to have differential effects on the pathogenesis of AD; and the absence of longitudinal data relating fibrillar Aβ to subsequent rates of cognitive decline or progression to MCI or AD. Whereas PiB binds to both parenchymal and cerebrovascular Aβ (i.e., cerebrovascular angiopathy), recent findings suggest that vascular Aβ is associated with

Table 2. Location and magnitude of maximally significant relationships between fibrillar Aβ burden and *APOE* ε4 gene dose

| | | Heterozygotes > noncarriers | | | | | Homozygotes > noncarriers | | | | | *APOE* ε4 gene dose | | | | |
| | | Atlas coordinates | | | | | Atlas coordinates | | | | | Atlas coordinates | | | | |
		X	Y	Z	z-score	P value	X	Y	Z	z-score	P value	X	Y	Z	z-score	P value
Anterior cingulate/frontal	L	−8	26	13	4.1	4e-4	−6	29	2	4.7	2e-5*	−4	26	13	5.6	4e-6*
	R	36	46	27	3.8	7e-4	32	56	−10	4.7	2e-5*	6	27	6	5.2	1e-5*
Mid-cingulate/posterior cingulate/precuneus	L	−4	−53	25	3.5	1e-3	−2	−58	36	4.1	1e-4*	−2	−14	30	4.4	9e-5*
	R	14	0	30	3.7	9e-4	2	19	29	4.0	1e-4*	2	19	29	4.2	1e-4*
Lateral temporal	L						−44	−44	−21	3.6	5e-4*	−46	−46	−21	3.7	5e-4*
	R	59	7	−17	3.5	1e-3	55	−13	−26	5.0	8e-6*	57	−9	−30	6.0	1e-6*
Basal ganglia	L	−6	−17	8	4.7	1e-4*	−2	−19	8	3.6	5e-4*	−10	12	30	5.3	9e-6*
	R						20	−2	−7	4.1	1e-4*	10	19	−8	4.4	8e-5*
Medial temporal	L						−12	−2	−10	3.6	5e-4*	−10	−6	−10	5.0	2e-5*
	R						22	−2	−10	4.2	1e-4*	20	−6	−10	4.2	1e-4*
Lateral parietal/parietotemporal	L						−55	−37	31	3.0	3e-3*	−57	−15	15	3.7	5e-4*
	R	57	−27	42	3.8	7e-4	48	−26	23	3.7	3e-4*	46	−24	23	4.0	2e-4*
Occipital/occipitotemporal	L						−42	−68	29	3.1	2e-3					
	R						44	−25	−26	4.4	5e-5*	32	−10	37	4.5	7e-5*

The data were extracted from voxels associated with maximally significant cerebral-to-cerebellar PiB DVR increases in the cognitively normal *APOE* ε4 homozygote versus noncarrier and heterozygote versus noncarrier comparisons (using the 2-tailed *t*-test) and in association with *APOE* ε4 gene dose (using 2-tailed linear trends). Listed locations correspond to the brain maps shown in Fig. 2 *A–C* and correspond to $P \le .005$, uncorrected for multiple comparisons. Asterisks denote locations that remain significant after correction for multiple comparisons (familywise error), based on random field theory within the ROI. Atlas coordinates were obtained from Talairach and Tournoux (41). X is the distance to the right (+) or left (−) of the midline, Y is the distance anterior (+) or posterior (−) to the anterior commissure, and Z is the distance superior (+) or inferior (−) to a horizontal plane through the anterior and posterior commissures.

greater PiB binding in occipital cortex than in other brain regions (31, 32). Whereas the brain maps in Fig. 2 use an unusually low *P* value threshold to visualize the distribution of increases in fibrillar Aβ, these changes are unlikely to reflect type I errors, for 3 reasons: the absence of cerebral voxels demonstrating PiB DVR increases in the opposing comparisons, the findings given in Table 2 using more conservative thresholds, and the symmetrical pattern of PiB DVR increases in regions expected to be preferentially affected by AD.

We have not yet analyzed the relationship between fibrillar Aβ burden and fluorodeoxyglucose PET measurements of cerebral metabolism, which we previously found to be inversely associated with *APOE ε4* gene dose. In addition, we have not yet investigated the relationship between fibrillar Aβ burden and other suggested risk factors for AD. Finally, we did not acquire the cerebrospinal fluid (CSF) samples necessary to determine how our findings might be related to CSF measurements of tau or Aβ$_{42}$, the main constituents of neurofibrillary tangles and plaques, respectively.

In a previous study, increased cerebral PiB binding was found to be associated with lower CSF Aβ$_{42}$ concentrations (33), supporting the use of either measurement as an indicator of fibrillar Aβ burden. In studies of nondemented older adults, higher CSF tau:Aβ$_{42}$ ratios were associated with higher rates of subsequent progression to the clinical stages of AD (34). The findings from these and other studies suggest that brain imaging and CSF measurements have complementary roles in the presymptomatic detection and tracking of AD. For instance, our brain imaging findings complement those from a CSF study of cognitively normal subjects age 59 ± 8 years, most (but not all) of whom had a first-degree family history of AD (35). In that study, lower CSF Aβ$_{42}$ levels were found in *APOE ε4* carriers compared with noncarriers and were associated with *APOE ε4* gene dose. The same study failed to detect significantly elevated CSF total tau levels in the *APOE ε4* carriers with low CSF Aβ$_{42}$ levels, raising the possibility that Aβ$_{42}$ precedes tau changes in the presymptomatic course of AD.

Although our study demonstrates an association between fibrillar Aβ and *APOE ε4* gene dose, PiB PET and other fibrillar Aβ imaging techniques are not yet recommended clinically to predict a healthy person's risk for AD. The extent to which fibrillar Aβ predicts whether or when a person might develop the clinical symptoms of AD, the extent to which it is associated with risk of AD in *APOE ε4* noncarriers, and the extent to which advantages of predicting a healthy person's risk outweigh any psychosocial disadvantages or the procedural costs remain to be clarified.

Longitudinal studies show promise in helping determine the extent to which fibrillar Aβ, alone or in combination with other measurements and risk factors, can predict subsequent rates of cognitive decline and progression to the clinical stages of AD. Our longitudinal study will ultimately permit us to characterize and compare rates of fibrillar Aβ progression in cognitively normal ε4 homozygotes, heterozygotes, and noncarriers. Additional studies are needed to further characterize, compare, and combine the roles of fibrillar Aβ imaging, CSF measurements, and other biomarkers in the presymptomatic detection and tracking of fibrillar Aβ, the assessment of other suggested AD risk factors, and the accelerated evaluation of promising risk-reducing and prevention therapies.

We have proposed the use of fibrillar Aβ imaging and other biomarkers to help evaluate the effectiveness of investigational treatments to reverse or slow their progression in cognitively normal people at unusually high risk for AD who are close to their anticipated age of onset of symptoms (24). If the effect of these treatments on fibrillar Aβ, alone or in combination with their effect on other brain imaging, CSF, or other biomarker measurements, can predict subsequent clinical decline, then these biomarker measurements might meet regulatory agency
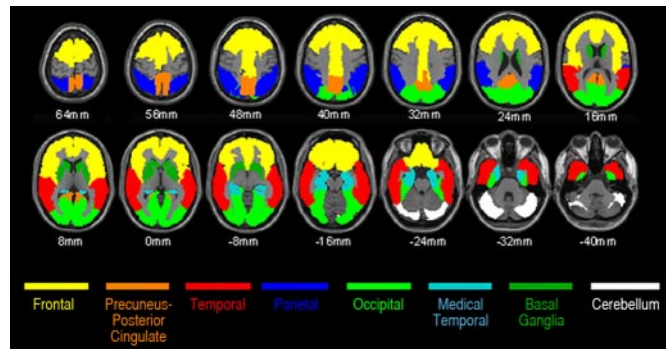
Fig. 3. Mean cortical PiB DVR (our primary outcome measure) generated using the frontal (including middle cingulate), posterior cingulate-precuneus, and lateral temporal ROIs.

criteria as reasonably likely surrogate endpoints, aiding the search for effective risk-reduction and prevention therapies ("presymptomatic AD treatments") as quickly as possible.

In summary, fibrillar Aβ burden is related to *APOE ε4* gene dose, but lower than that in clinically affected AD patients, in cognitively normal subjects before their estimated mean age at onset of dementia. These findings support the possibility of using fibrillar Aβ imaging, along with other biomarkers of Aβ, tau, and neuronal pathology and other risk factors, in the preclinical detection and tracking of AD and the evaluation of promising prevention therapies.

Materials and Methods

Study Design. PiB PET was performed in the first 29 returning *APOE ε4* homozygotes, heterozygotes, and noncarriers in our longitudinal cohort study. Newspaper advertisements were originally used to recruit volunteers, ranging in age from 47 to 68 years (mean age, 56 ± 5 years) who denied memory concerns, reported a first-degree family history of AD, and agreed to not receive information about their *APOE* genotype. All subjects provided informed consent, and the study was conducted following guidelines approved by the Human Subjects Committees at Banner Health and the Mayo Clinic. *APOE* genotypes were characterized from venous blood samples (36). *APOE ε4* homozygotes, heterozygotes, and noncarriers who were similar in terms of sex, age, and educational level and who had an MMSE (37) score ≥ 28 at their first visit were assessed every 2 years in an ongoing longitudinal study using clinical ratings, neuropsychological tests, volumetric MRI, and fluorodeoxyglucose PET, as described previously (17–20). Whereas some of the study subjects were enrolled as early as 1993, PiB PET was not introduced into the study until 2008. At the time of their PiB PET scans, 28 of the returning subjects were cognitively normal, including 8 ε4 homozygotes, 8 heterozygotes (all with the ε3/ε4 genotype), and 12 noncarriers (7 with the ε3/ε3 genotype and 1 with the ε2/ε3 genotype). These subjects' demographic characteristics, MMSE scores, and neuropsychological scores are given in Table 1. The mean ages of the homozygote, heterozygote, and noncarrier groups were younger than the mean age at clinical onset in each of the respective genetic groups in the original case-control study (14). A ninth ε4 homozygote (age 73 years) developed subjective and neuropsychological evidence of cognitive decline in the 2 years between her last 2 clinical visits, and she was diagnosed with amnestic MCI (38) 7 months before her PiB PET scan.

To relate the magnitude and distribution of our fibrillar Aβ measurements to those observed in AD dementia, we subsequently analyzed fibrillar Aβ PET data from 10 probable AD patients from a previous study (11). These patients included 5 ε4 homozygotes, 4 heterozygotes, and 1 noncarrier (mean age, 69 ± 8 years; range 55–77 years; mean MMSE, 22.9 ± 3).

Fibrillar Aβ Imaging. Fibrillar Aβ imaging was performed in the returning *APOE ε4* homozygotes, heterozygotes, and noncarriers at the Banner Alzheimer's Institute using a Siemens HR+ scanner in the 3-dimensional mode, a transmission scan, the i.v. injection of 15 mCi of ^{11}C-PiB, and a 90-min dynamic sequence of emission scans. Similarly, fibrillar Aβ imaging was performed previously in the probable AD patients at the University of Pittsburgh using an HR+ scanner and a 90-min dynamic sequence of emission scans. Each person's PET image was reconstructed using a back-projection method, with correction

for radiation scatter and attention, and a Hanning filter. The data were converted to cerebral-to-cerebellar PiB DVR, a measure of fibrillar Aβ burden, using images from the 40- to 90-min emission frames, an automatically labeled cerebellar reference region, and the Logan method. The Logan method was used on a regional basis to characterize and compare PiB DVRs in preselected ROIs and on a voxel-by-voxel basis to generate PiB DVR images and statistical maps (6, 8, 39).

Regions of Interest. The automatic anatomic labeling algorithm (40) was used to characterize PiB DVRs in preselected frontal, posterior cingulate-precuneus, lateral temporal, lateral parietal, and basal ganglia ROIs, which are preferentially affected in AD, and in medial temporal and occipital ROIs, which are less severely affected in AD (Fig. 3). For our primary comparison, a mean cortical ROI consisting of frontal, posterior cingulate-precuneus, and lateral temporal ROIs also was defined. Using the published list of automatically labeled regions, the frontal ROI included bilateral frontal, anterior cingulate, middle cingulate, and insular cortex regions 3–34; the posterior cingulate-precuneus ROI included bilateral regions 35–36 and 67–68; the lateral temporal ROI included bilateral regions 79–90; the lateral parietal ROI included bilateral regions 59–65; the basal ganglia ROI included bilateral caudate, putamen, and globus pallidus regions 71–76; the medial temporal ROI included bilateral hippocampus, parahippocampal gyrus, and amygdala regions 37–42; the occipital ROI included bilateral regions 43–56; and the cerebellar reference ROI included bilateral cerebellar crus I regions 91–92. Fig. 1 shows mean cortical and ROI PiB DVRs from the cognitively normal APOE ε4 noncarriers, heterozygotes, and homozygotes (white box), the ε4 homozygote with MCI, and the reference probable AD patients (gray box). The homozygotes' mean value in the figure and statistical analyses in the text do not include data from the subject with MCI. The P values in the figure correspond to the association between fibrillar Aβ burden and APOE ε4 gene dose (2-tailed linear trend) in the cognitively normal subjects.

We recently used an iterative procedure to identify outliers in a group of cognitively unimpaired older controls (11), and we proposed characterizing subjects as PiB-positive if their measurements exceeded a minimum threshold in at least one AD-affected ROI. For this study, we used a PiB DVR of at least 1.40 in at least 1 of the AD-affected cortical, frontal, posterior cingulate-precuneus, temporal, parietal, and basal ganglia ROIs. This predefined threshold was based on a reanalysis of the previous older control data (11) with no correction for the combined effects of brain atrophy and partial-volume averaging, elimination of the occipital ROI to minimize the contribution of vascular Aβ to this assessment (31), and application of a single threshold to all of the ROIs.

Statistical Brain Mapping. A brain-mapping algorithm (SPM5; http://www.fil.ion.ucl.ac.uk/spm/), PiB DVR images from the cognitively normal subjects (not including the homozygote with MCI), and spatial information from their 3.5- to 10-min emission frames were used to automatically normalize the images according to the coordinates of a standard brain atlas (41), to smooth the images to 12 mm full-width-at-half-maximum, and to generate statistical parametric maps of APOE ε4 gene dose–related PiB DVR differences and associations (Fig. 2 A–C).

1. Hardy J, Selkoe DJ (2002) The amyloid hypothesis of Alzheimer's disease: Progress and problems on the road to therapeutics. *Science* 297:353–356.
2. Price JL, Morris JC (1999) Tangles and plaques in nondemented aging and ''preclinical'' Alzheimer's disease. *Ann Neurol* 45:358–368.
3. Oddo S, Billings L, Kesslak JP, Cribbs DH, LaFerla FM (2004) Abeta immunotherapy leads to clearance of early, but not late, hyperphosphorylated tau aggregates via the proteasome. *Neuron* 43:321–332.
4. Dickson DW, et al. (1992) Identification of normal and pathological aging in prospectively studied nondemented elderly humans. *Neurobiol Aging* 13:179–189.
5. Bennett DA, et al. (2006) Neuropathology of older persons without cognitive impairment from two community-based studies. *Neurology* 66:1837–1844.
6. Klunk WE, et al. (2004) Imaging brain amyloid in Alzheimer's disease with Pittsburgh Compound-B. *Ann Neurol* 55:306–319.
7. Ikonomovic MD, et al. (2008) Post-mortem correlates of in vivo PiB-PET amyloid imaging in a typical case of Alzheimer's disease. *Brain* 131:1630–1645.
8. Lopresti BJ, et al. (2005) Simplified quantification of Pittsburgh Compound B amyloid imaging PET studies: A comparative analysis. *J Nucl Med* 46:1959–1972.
9. Mintun MA, et al. (2006) [11C]PIB in a nondemented population: Potential antecedent marker of Alzheimer disease. *Neurology* 67:446–452.
10. Rowe CC, et al. (2007) Imaging beta-amyloid burden in aging and dementia. *Neurology* 68:1718–1725.
11. Aizenstein HJ, et al. (2008) Frequent amyloid deposition without significant cognitive impairment among the elderly. *Arch Neurol* 65:1509–1517.
12. Forsberg A, et al. (2008) PET imaging of amyloid deposition in patients with mild cognitive impairment. *Neurobiol Aging* 29:1456–1465.
13. Strittmatter WJ, et al. (1993) Apolipoprotein E: High-avidity binding to beta-amyloid and increased frequency of type 4 allele in late-onset familial Alzheimer disease. *Proc Natl Acad Sci U S A* 90:1977–1981.
14. Corder EH, et al. (1993) Gene dose of apolipoprotein E type 4 allele and the risk of Alzheimer's disease in late-onset families. *Science* 261:921–923.
15. Farrer LA, et al. (1997) Effects of age, sex, and ethnicity on the association between apolipoprotein E genotype and Alzheimer disease: A meta-analysis. APOE and Alzheimer Disease Meta Analysis Consortium. *JAMA* 278:1349–1356.
16. Coon KD, et al. (2007) A high-density whole-genome association study reveals that APOE is the major susceptibility gene for sporadic late-onset Alzheimer's disease. *J Clin Psychiatry* 68:613–618.
17. Reiman EM, et al. (1996) Preclinical evidence of Alzheimer's disease in persons homozygous for the ε4 allele for apolipoprotein E. *N Engl J Med* 334:752–758.
18. Reiman EM, Caselli RJ, Alexander GE, Chen K (2001) Tracking the decline in cerebral glucose metabolism in persons and laboratory animals at genetic risk for Alzheimer's disease. *Clin Neurosci Res* 1:194–206.
19. Reiman EM, et al. (2001) Declining brain activity in cognitively normal apolipoprotein E ε4 heterozygotes: A foundation for using positron emission tomography to efficiently test treatments to prevent Alzheimer's disease. *Proc Natl Acad Sci U S A* 98:3334–3339.
20. Reiman EM, et al. (2005) Correlations between apolipoprotein E ε4 gene dose and brain imaging measurements of regional hypometabolism. *Proc Natl Acad Sci U S A* 102:8299–8302.
21. Reiman EM, et al. (2004) Functional brain abnormalities in young adults at genetic risk for late-onset Alzheimer's dementia. *Proc Natl Acad Sci U S A* 101:284–289.
22. Klunk WE, et al. (2007) Amyloid deposition begins in the striatum of presenilin-1 mutation carriers from two unrelated pedigrees. *J Neurosci* 27:6174–6184.
23. Reiman EM, et al. (2008) Cholesterol-related genetic risk scores are associated with hypometabolism in Alzheimer's-affected brain regions. *Neuroimage* 40:1214–1221.
24. Reiman EM, Langbaum JBS (in press) in *Imaging and the Aging Brain*, eds. Jagust WJ, D'Esposito M (Oxford Univ Press, New York).
25. Schmechel DE, et al. (1993) Increased amyloid beta-peptide deposition in cerebral cortex as a consequence of apolipoprotein E genotype in late-onset Alzheimer disease. *Proc Natl Acad Sci U S A* 90:9649–9653.
26. Wisniewski T, Castano EM, Golabek A, Vogel T, Frangione B (1994) Acceleration of Alzheimer's fibril formation by apolipoprotein E in vitro. *Am J Pathol* 145:1030–1035.
27. Bales KR, Dodart JC, DeMattos RB, Holtzman DM, Paul SM (2002) Apolipoprotein E, amyloid, and Alzheimer disease. *Mol Interv* 2:363–375.
28. Koistinaho M, et al. (2004) Apolipoprotein E promotes astrocyte colocalization and degradation of deposited amyloid-beta peptides. *Nat Med* 10:719–726.
29. Jiang Q, et al. (2008) ApoE promotes the proteolytic degradation of Abeta. *Neuron* 58:681–693.
30. Risner ME, et al. (2006) Efficacy of rosiglitazone in a genetically defined population with mild-to-moderate Alzheimer's disease. *Pharmacogenomics J* 6:246–254.
31. Greenberg SM, et al. (2008) Detection of isolated cerebrovascular beta-amyloid with Pittsburgh compound B. *Ann Neurol* 64:587–591.
32. Johnson KA, et al. (2007) Imaging of amyloid burden and distribution in cerebral amyloid angiopathy. *Ann Neurol* 62:229–234.
33. Fagan AM, et al. (2006) Inverse relation between in vivo amyloid imaging load and cerebrospinal fluid Aβ42 in humans. *Ann Neurol* 59:512–519.
34. Fagan AM, et al. (2007) Cerebrospinal fluid tau/β-amyloid42 ratio as a prediction of cognitive decline in nondemented older adults. *Arch Neurol* 64:343–349.
35. Sunderland T, et al. (2004) Cerebrospinal fluid beta-amyloid1–42 and tau in control subjects at risk for Alzheimer's disease: The effect of APOE epsilon4 allele. *Biol Psychiatry* 56:670–676.
36. Hixson JE, Vernier DT (1990) Restriction isotyping of human apolipoprotein E by gene amplification and cleavage with HhaI. *J Lipid Res* 31:545–548.
37. Folstein MF, Folstein SE, McHugh PR (1975) ''Mini-mental state'': A practical method for grading the cognitive state of patients for the clinician. *J Psychiatr Res* 12:189–198.
38. Winblad B, et al. (2004) Mild cognitive impairment: Beyond controversies, towards a consensus. Report of the International Working Group on Mild Cognitive Impairment. *J Intern Med* 256:240–246.
39. Price JC, et al. (2005) Kinetic modeling of amyloid binding in humans using PET imaging and Pittsburgh Compound-B. *J Cereb Blood Flow Metab* 25:1528–1547.
40. Tzourio-Mazoyer N, et al. (2002) Automated anatomical labeling of activations in SPM using a macroscopic anatomical parcellation of the MNI MRI single-subject brain. *Neuroimage* 15:273–289.
41. Talairach J, Tournoux P (1988) *Co-Planar Stereotaxic Atlas of the Human Brain* (Thieme, New York).

NEUROSCIENCE

www.manaraa.com